HHS Public Access

Author manuscript

Mol Pharm. Author manuscript; available in PMC 2022 July 06.

Published in final edited form as:

Mol Pharm. 2021 March 01; 18(3): 1238–1246. doi:10.1021/acs.molpharmaceut.0c01107.

Fluorescence Imaging of Tumor-Accumulating Antibody-IR700 Conjugates Prior to Near-Infrared Photoimmunotherapy (NIR-PIT) Using a Commercially Available Camera Designed for Indocyanine Green

Fuyuki F. Inagaki,
Molecular Imaging Branch, Center for Cancer Research, National Cancer Institute, National Institutes of Health, Bethesda, Maryland 20892, United States

Daiki Fujimura,
Molecular Imaging Branch, Center for Cancer Research, National Cancer Institute, National Institutes of Health, Bethesda, Maryland 20892, United States

Aki Furusawa,
Molecular Imaging Branch, Center for Cancer Research, National Cancer Institute, National Institutes of Health, Bethesda, Maryland 20892, United States

Ryuhei Okada,
Molecular Imaging Branch, Center for Cancer Research, National Cancer Institute, National Institutes of Health, Bethesda, Maryland 20892, United States

Hiroaki Wakiyama,
Molecular Imaging Branch, Center for Cancer Research, National Cancer Institute, National Institutes of Health, Bethesda, Maryland 20892, United States

Takuya Kato,
Molecular Imaging Branch, Center for Cancer Research, National Cancer Institute, National Institutes of Health, Bethesda, Maryland 20892, United States

Peter L. Choyke,
Molecular Imaging Branch, Center for Cancer Research, National Cancer Institute, National Institutes of Health, Bethesda, Maryland 20892, United States

Hisataka Kobayashi
Molecular Imaging Branch, Center for Cancer Research, National Cancer Institute, National Institutes of Health, Bethesda, Maryland 20892, United States

Abstract

Near-infrared photoimmunotherapy (NIR-PIT) is a newly developed cancer treatment that uses antibody-IRDye700DX (IR700) conjugates and was recently approved in Japan for patients with

Corresponding Author: Hisataka Kobayashi – Phone: 240-858-3069; kobayash@mail.nih.gov; Fax: 240-541-4527.

The authors declare no competing financial interest.

Complete contact information is available at: https://pubs.acs.org/10.1021/acs.molpharmaceut.0c01107

inoperable head and neck cancer. Exposure of the tumor with NIR light at a wavelength of 690 nm leads to physicochemical changes in the antibody-IR700 conjugate–cell receptor complex, resulting in increased hydrophobicity and damage to the integrity of the cell membrane. However, it is important that the tumor be completely exposed to light during NIR-PIT, and thus, a method to provide real-time information on tumor location would help clinicians direct light more accurately. IR700 is a fluorophore that emits at 702 nm; however, there is no clinically available device optimized for detecting this fluorescence. On the other hand, many indocyanine green (ICG) fluorescence imaging devices have been approved for clinical use in operating rooms. Therefore, we investigated whether LIGHTVISION, one of the clinically available ICG cameras, could be employed for NIR-PIT target tumor detection. Due to the limited benefits of adding IR700 molecules, the additional conjugation of IRDye800CW (IR800) or ICG-EG4-Sulfo-OSu (ICG-EG4), which has an overlapping spectrum with ICG, to trastuzumab-IR700 conjugates was performed. Conjugation of second NIR dyes did not interfere the efficacy of NIR-PIT. The dual conjugation of IR800 and IR700 to trastuzumab clearly visualized target tumors with LIGHTVISION by detecting emission light of IR800. We demonstrated that the conjugation of second NIR dyes enables us to provide a real-time feedback of tumor locations prior to NIR-PIT.

Graphical Abstract

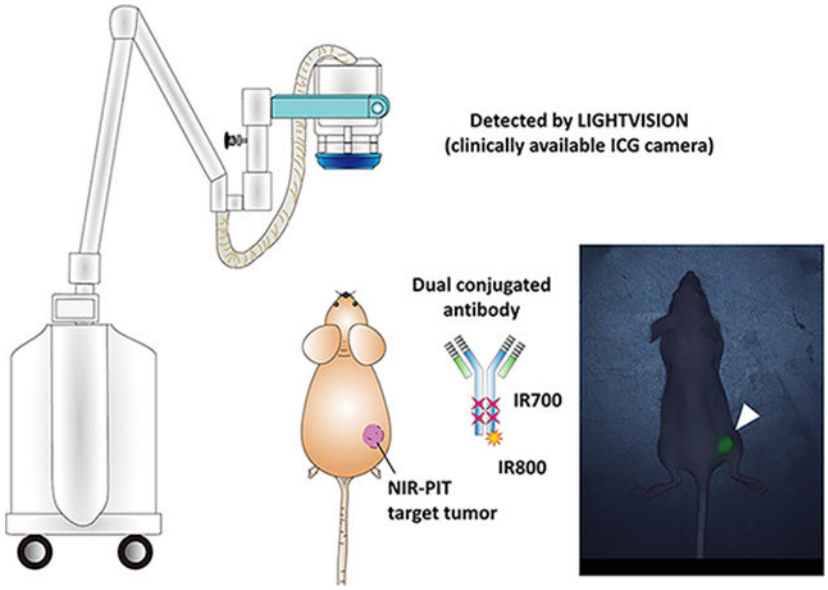

Keywords

near-infrared photoimmunotherapy; optical imaging; IR700; near-infrared camera; indocyanine green

INTRODUCTION

Near-infrared photoimmunotherapy (NIR-PIT) is a newly developed cancer therapy, which utilizes an antibody labeled with an NIR photon-absorbing silicon phthalocyanine dye, IRDye700DX (IR700). An antibody-photoabsorber conjugate (APC) specifically binds to

antigen-expressing cells, and subsequent exposure to NIR light (approximately 690 nm) selectively injures the cell membrane, wherever the conjugate is bound, leading to necrotic cell death.[1–4] This concept has been used with a variety of antibodies and tumor types.[5–9] A phase 1/2 clinical trial using EGFR-targeted cetuximab-IR700 (ASP-1929) in patients with inoperable head and neck cancer showed a high response rate (https://clinicaltrials.gov/ct2/show/NCT02422979) and received qualified approval from the Japanese Ministry of Health, Labor and Welfare in September 2020 and Fast Track designation from the U.S. Food and Drug Administration (FDA). Currently, a global phase 3 clinical trial is underway (https://clinicaltrials.gov/ct2/show/NCT03769506).

NIR-PIT requires that light be applied to the entire tumor. However, it can be difficult to locate a tumor while in a procedure suite. Pretreatment imaging modalities such as computed tomography (CT), magnetic resonance imaging (MRI), and positron emission tomography (PET) provide detailed information about tumor location prior to treatment, but during treatment, options are limited. Therefore, fluorescence imaging is expected as an intratreatment diagnostic modality, which can provide real-time information about tumor location.[10] Indocyanine green (ICG), methylene blue, and 5-ALA are FDA-approved fluorescence dyes. Among them, ICG is the most successful dye because of its low toxicity and deeper tissue penetration and has specifically been employed to identify extrahepatic bile ducts, liver tumors, and sentinel lymph nodes.[11–13] As a result of its properties, several commercially available imaging systems for ICG have been developed.

IR700 is a fluorescence dye that emits light with a wavelength of around 700 nm, when irradiated with light with a wavelength of around 690 nm. However, there is no clinically available imaging device that is optimized for detection of IR700 fluorescence. Therefore, there will be an increasing demand for procedures that can be used to visualize target tumors in clinical settings. The purpose of this study was to demonstrate the feasibility of intratreatment tumor detection using clinically available imaging hardware (LIGHTVISION) originally designed for ICG imaging. We added IR800 or ICG-EG4-Sulfo-OSu (ICG-EG4) to trastuzumab-IR700 conjugates and demonstrated visualization of the tumor. This method can achieve real-time feedback of tumor locations prior to NIR-PIT.

MATERIALS AND METHODS

Reagents.

IRDye700DX NHS ester (IR700) and IRDye800CW NHS ester (IR800) were purchased from LI-COR Bioscience (Lincoln, NE). ICG-EG4-Sulfo-OSu (ICG-EG4) was purchased from Dojindo Molecular Technologies (Rockville, MD). Trastuzumab, 95% humanized monoclonal antibody against human epidermal growth factor receptor type 2 (HER2), was purchased from Genentech (South San Francisco, CA). All other chemicals were of reagent grade.

Synthesis of Antibody–Dye Conjugate.

Conjugation of dye with monoclonal antibody was performed as previously described.[14] In brief, trastuzumab (1 mg, 6.8 nmol) was incubated with IR700 (34.2 nmol, 10 mmol/L in

DMSO), and IR800 (17.1 nmol, 5 mmol/L in DMSO) or ICG-EG4 (17.1 nmol, 5 mmol/L in DMSO) in 0.1 mol/L Na_2HPO_4 (pH 8.5) at room temperature for 60 min. The reactant was purified with a gel filtration column (Sephadex G 25 column, PD-10, GE Healthcare, Piscataway, NJ). We abbreviate IR700 conjugated to trastuzumab as Tra-IR700. IR700 and IR800 dual-conjugated to trastuzumab and IR700 and ICG-EG4 dual-conjugated to trastuzumab are abbreviated as Tra-IR700/IR800 and Tra-IR700/ICG-EG4, respectively. For experiments on IR700 loading, six samples with different IR700:trastuzumab mixing molar ratios (0:1, 0.5:1, 1:1, 2.5:1, 5:1, 10:1, 20:1) were prepared.

SDS-PAGE.

The number of covalently conjugated dyes with each antibody was quantified by the UV–Vis system (8453 Value UV–Vis system, Agilent Technologies, Santa Clara, CA) and SDS-PAGE. The absorption at 280, 689, and 779 nm of each conjugate was measured by the UV–Vis system. Each conjugate was separated by SDS-PAGE with a 4–20% gradient polyacrylamide gel (Life Technologies, Gaithersburg, MD). After electrophoresis at 80 V for 100 min, the gel was imaged with a Pearl Imager (LI-COR Biosciences, Lincoln, NE) using an IR700 fluorescence channel (excitation wavelength: 685 nm, collection wavelength: 720 nm) and a fluorescence channel (excitation wavelength: 785 nm, collection wavelength: 820 nm). Fluorescence intensity of the band was measured with Pearl Cam Software (LI-COR Bioscience). The gel was stained with colloidal blue staining to confirm the antibody band.

Size-Exclusion Chromatography.

Size-exclusion chromatography (SEC) analysis was performed on the Nexera XR UHPLC system (Shimadzu Co., Kyoto, Japan), as previously reported.[14] Briefly, approximately 25 μg of protein was loaded onto a TSKgel SuperSW 3000 (4.6 mm × 30 cm, 5 μm) with a guard column (Tosoh Bioscience, Inc., South San Francisco, CA) and eluted using an isocratic flow (37 min, 0.25 mL/min) of 200 mM sodium phosphate with 10% acetonitrile at pH 6.8. The absorption of elution was monitored at a wavelength of 280 and 689 nm with the SPD-M30A photodiode array detector. The emission of the elution (excitation: 689 nm) was monitored at a wavelength of 700 nm with the RF-20Axs fluorescence detector.

Cell Culture.

A human gastric cancer cell line, N87-GFP/luc, and a transformed murine fibroblast cell line, Balb/3T3, were used in this study. N87-GFP/luc cells were cultured in an RPMI 1640 medium (GIBCO, Waltham, MA) supplemented with 10% FBS (GIBCO, Waltham, MA) and 1% penicillin/streptomycin (GIBCO, Waltham, MA) in a humidified incubator in an atmosphere of 95% air and 5% carbon dioxide. Balb/3T3 cells were cultured in a DMEM medium (GIBCO) supplemented with 10% FBS and 1% penicillin/streptomycin in a humidified incubator in an atmosphere of 95% air and 5% carbon dioxide.

Flow Cytometric Analysis of HER2 Expression.

N87-GFP/luc cells or Balb/3T3 cells (1×10^6) were incubated with 1 μg of Tra-IR700 for 1 h on ice. After washing with PBS, cells were analyzed by FACSLyric (BD Biosciences) and FlowJo Software (BD Biosciences).

In Vitro NIR-PIT.

The cytotoxic effects of NIR-PIT were determined by flow cytometric analysis. N87-GFP/luc cells (2×10^5) were seeded into 12-well plates and cultured for 2 days. The medium was replaced with a fresh culture medium containing 10 μg/mL of APC and incubated for 3 h at 37°C. After washing with PBS, cells were irradiated with an NIR-laser (690 nm) at indicated energy densities (ML7710, Modulight Inc). Cells were detached 1 h after irradiation and propidium iodide (PI) was added. Samples were analyzed by FACSCalibur (BD Biosciences) and CellQuest Software (BD Biosciences). Balb/3T3 cells (2×10^5) were seeded into 12-well plates and cultured for 1 day. The medium was replaced with a fresh culture medium containing 10 μg/mL of APC and incubated for 3 h at 37°C. Without washing, cells were irradiated with an NIR-laser (690 nm) at indicated energy densities. Cells were detached 1 h after irradiation and PI was added. Samples were analyzed by FACSLyric and BD FACSuite Software (BD Biosciences). In APC-dose-dependent experiments, APC was added to the medium at an indicated concentration, and cells were irradiated with an NIR-laser at a 16 J/cm^2 energy density. In experiments on IR700 loading, the culture medium containing 10 μg/mL of APC was added, and cells were irradiated with an NIR-laser at an 8 J/cm^2 energy density.

Animal Models.

All animal procedures were performed in compliance with the Guide for the Care and Use of Laboratory Animal Resources (1996), the National Research Council, and approved by the local Animal Care and Use Committee. Female homozygote athymic nude mice were used (Charles River, NCI-Frederick, Frederick, MD). During the procedure, mice were anesthetized with the inhalation of 2.5–4.0% isoflurane. In the subcutaneous tumor model, 3×10^6 N87-GFP/luc cells were subcutaneously injected into the right lower flank of mice. When tumors reached 7–9 mm in longer diameter, mice were used for the following imaging studies.

Fluorescence Imaging.

Hundred micrograms of APC was administered intravenously the day before the imaging experiment. IR700 and IR800 fluorescent images wer obtained with the Pearl Imager (LI-COR Bioscience) using an IR700 fluorescence channel and an IR800 fluorescence channel. For analyzing fluorescence intensities, regions of interest (ROIs) were manually drawn on the tumor. As background, ROIs were manually drawn on the opposite side from the tumor. The average fluorescence intensities of each ROI were measured by Pearl Cam Software (LI-COR Bioscience). The target-to-background ratio (TBR) was calculated by the following equation: TBR = (fluorescence intensity of the target) / (fluorescence intensity of the background). The LIGHTVISION imaging system (Shimadzu Corp., Kyoto, Japan) was also used to obtain fluorescent images (excitation wavelength: 780–800 nm, collection wavelength: 800–850 nm). The camera was placed 50 cm from the recording surface, and detector sensitivity to ICG was set to 22. The obtained images were analyzed by Fiji Software.[15]

In Vivo NIR-PIT.

Hundred micrograms of APC was administered via the tail vein the day before the experiment. Tumors were irradiated with an NIR-laser (690 ± 5 nm) at a 50 J/cm^2 energy density (ML7710, Modulight, Inc. Tampere, Finland). Before and after irradiation, fluorescent images were obtained with the Pearl Imager and LIGHTVISION. For bioluminescence imaging (BLI), D-luciferin (15 mg/mL, 200 μL) (Gold Biotechnology, St. Louis, MO) was injected intraperitoneally, and bioluminescence images were obtained with Photon Imager (Biospace Lab, Nesles la Vallee, France), 15 min after injection. ROIs were placed over the entire tumor. The counts per minute of relative light units were calculated using M3 Vision Software (Biospace Lab) and converted to the percentage decrease in light based on a comparison of post NIR-PIT to pretreatment BLI using the following formula: [(relative light units after treatment)/(relative light units before treatment) × 100 (%)].

Pathological Analysis.

One day after NIR-PIT, tumors were resected and fixed with 10% neutral-buffered formaldehyde. Paraffin-embedded sections were stained with hematoxylin and eosin (H&E). Photomicrographs were acquired using an Olympus BX43 microscope (Olympus, Tokyo, Japan).

Statistical Analysis.

Statistical analysis was performed with GraphPad Prism version 7 software (GraphPad Software, La Jolla, CA). Data were presented as the mean ± standard error of mean (SEM) from a minimum of four experiments, unless otherwise indicated. Student's *t* test was used for comparison between two groups. A one-way analysis of variance (ANOVA) followed by Tukey's correction was used for comparison among three groups. A *p*-value of less than 0.05 was considered statistically significant.

RESULTS

Factors That Determine the Efficacy of NIR-PIT.

First, we examined the factors that determined the therapeutic effect of Tra-IR700 NIR-PIT using N87-GFP/luc cells and Balb/3T3 cells. While Tra-IR700 bound to HER2 expressing N87-GFP/luc cells, Tra-IR700 did not bind to HER2-negative Balb/3T3 cells (Figure 1A). As mentioned in previous reports, HER2-positive N87-GFP/luc cells were injured by Tra-IR700 NIR-PIT. The therapeutic effect of NIR-PIT increased as the amount of NIR light exposure increased (Figure 1B).[16] On the other hand, HER2-negative Balb/3T3 cells were not damaged by Tra-IR700 NIR-PIT even in the presence of unbinding APCs (Figure 1C). These results showed that only APCs bound to the cell membrane had the ability of cell killing. Further, the therapeutic effect increased as the APC dose increased (Figure 1D). Next, we examined whether the number of IR700 conjugated to trastuzumab affected the therapeutic effect of NIR-PIT. The absorption at 689 nm of Tra-IR700 increased linearly as the dye/protein mixing ratio increased, indicating that IR700 is bound to trastuzumab (Figure 1E). When the IR700 loading was small, the therapeutic effect increased as the number increased. However, the therapeutic effect reached a ceiling at a 1:5 mixing ratio

(Figure 1F). This means that there is a limit beyond which additional conjugated dyes do not add to the therapeutic effect. This phenomenon has also been reported in panitumumab-IR700.[14]

Characteristics of Dual-Conjugated Antibody.

As can be seen from the result of Figure 1F, excessive IR700 loading did not enhance the therapeutic effect of NIR-PIT. We hypothesized that we could add other types of dyes such as IR800 or ICG-EG4 to trastuzumab without negating the therapeutic effect of the bound IR700 (Figure 2A). Reacting trastuzumab with the mixture of IR700 and, IR800 or ICG-EG4, dual-conjugated antibodies were prepared. To evaluate the characteristics of dual-conjugated antibodies, SDS-PAGE was performed. The position of the fluorescence signal of IR700 and IR800 or ICG-EG4 coincided with the position of the antibody band on SDS-PAGE (Figure 2B). The number of dyes conjugated to each antibody was calculated with light absorption at 280, 689, and 778 nm in the UV–vis system and the fluorescence intensity ratio of each band in SDS-PAGE. The number of covalently conjugated IR700 in Tra-IR700 was 3.75 ± 0.09. The number of covalently conjugated IR700 and IR800 in Tra-IR700/IR800 was 3.88 ± 0.22 and 1.52 ± 0.14, respectively. The number of covalently conjugated IR700 and ICG-EG4 in Tra-IR700/ICG was 3.81 ± 0.12 and 1.55 ± 0.11, respectively. We investigated whether the additional conjugation of IR800 or ICG affected the efficacy of *in vitro* NIR-PIT. There was no significant difference in cell viability among Tra-IR700-, Tra-IR700/IR800-, and Tra-IR700/ICG-EG4-treated cells (Figure 2C).

Comparison of Tra-IR700/IR800 and Tra-IR700/ICG-EG4.

Next, we performed imaging studies in N87-GFP/luc tumor-bearing mice administered Tra-IR700/IR800 or Tra-IR700/ICG-EG4, using the Pearl Imager and LIGHTVISION (Figure 3A,B). LIGHTVISION is a commercially available approved device that can detect NIR fluorescence dye at a wavelength of around 800 nm and was designed mainly for ICG (Table 1). Tumor fluorescence measured by the 700 nm fluorescence channel of the Pearl Imager was similar between the two groups. The relative fluorescence intensity on the Pearl Imager of IR800 was more than 15 times that of ICG-EG4 (Figure 3A,C). In the images obtained by LIGHTVISION, the fluorescence of ICG-EG4 was hardly detected, whereas the fluorescence of IR800 was clearly detected (Figure 3B). The relative fluorescence intensity of IR800 was more than 100 times higher than that of ICG-EG4 (Figure 3D). In the images obtained with the Pearl Imager, there was no significant difference between the TBRs (6.2) of IR700 fluorescence and the TBRs (6.7) of IR800 fluorescence. When using LIGHTVISION, mean TBRs of 161.3 were observed, which were about 24 times higher than the TBRs obtained with the IR800 channel of the Pearl Imager (Figure 3E).

Fluorescence Change and Therapeutic Effect After In Vivo NIR-PIT.

Fluorescence images of Tra-IR700/IR800 were obtained with the Pearl Imager and LIGHTVISION before and after NIR-PIT (Figure 4A). After NIR-PIT, the fluorescence in the tumor was diminished and background fluorescence was also reduced due to light irradiation for APCs circulating in the blood. In the images obtained with the Pearl Imager, the degree of attenuation was greater in IR700 (Figure 4B) and mean TBRs of IR700 fluorescence were smaller than those of IR800 fluorescence (Figure 4C). No background

signal was detected in the images obtained with LIGHTVISION after NIR-PIT, and the TBRs could not be calculated (Figure 4C). Last, we examined whether the additional conjugation of IR800 affected the efficacy of in vivo NIR-PIT. To estimate tumor viability, BLI was performed before and 6 h after NIR-PIT. There was no significant difference in the attenuation rate of bioluminescence between the Tra-IR700 PIT group and Tra-IR700/IR800 PIT group (Figure 4D). Histology showed diffuse necrosis and microhemorrhage in the Tra-IR700 PIT group. Similar histological changes were also observed in the Tra-IR700/IR800 PIT group (Figure 4E).

DISCUSSION

Optical navigation is a powerful tool to identify cancerous tissues during procedures. Real-time feedback of tumor locations helps surgeons or endoscopists resect entire tumors while sparing normal tissues.[10] In NIR-PIT, to set the light irradiation field precisely, it is considered beneficial to provide real-time feedback of tumor locations. In this study, we showed that LIGHTVISION could detect NIR-PIT-targeted tumors by the conjugation of second NIR dyes.

The main mechanism of cell killing in NIR-PIT is the change in chemical properties of IR700 from hydrophilic to hydrophobic by NIR light irradiation. The increase in hydrophobicity leads to conformational change of the APC and physical damage to cell membranes.[17] There are more than 100 primary amine sites where IR700 NHS ester can be conjugated to an antibody. However, our data show that there is a limit to the benefits of adding additional IR700 molecules (Figure 1C). This is a unique feature of IR700, unlike most antibody–drug conjugates, which efficacy increases with increased payload. As the therapeutic effect of Tra-IR700 reached a maximum at the 5:1 mixing ratio (IR700:trastuzumab), additional conjugation of IR800 NHS ester or ICG-PEG4-Sulfo-OSu to empty primary amines was performed (Figure 2). ICG-PEG4-Sulfo-OSu is an ICG derivative with short polyethylene glycol linkers, which improves the percentage of covalently binding dye to antibody and TBRs compared to ICG-Sulfo-OSu.[18,19] It has an NIR absorption and emission peak of 789/814 nm. The components of ICG-EG4, indocyanine green, and PEG have been clinically used for many years and their toxicity profiles are known to be favorable for clinical use.[20,21] IRDye800CW is a cyanine-based dye, which has an NIR absorption and emission peak of 778/794 nm. IRDye800CW has not been approved by FDA but has been well examined in conjugation with antibodies.[22] Its feasibility and safety for surgical navigation have been reported in several phase I/II clinical studies in patients with head and neck cancer, breast cancer, and glioblastoma.[23–26] Because of the overlapping excitation and emission spectra with indocyanine green, LIGHTVISION (excitation wavelength: 780–800 mm, collection wavelength: 800–850 nm) was likely to detect both fluorescence dyes. The Pearl Imager was able to visualize N87-GFP/luc tumors with both Tra-IR700/IR800 and Tra-IR700/ICG-EG4, but the fluorescence intensity of ICG-EG4 was less than one-tenth of IR800 (Figure 3A,3C). LIGHTVISION was able to visualize tumors when using Tra-IR700/IR800, but it was unable to clearly visualize tumors when using Tra-IR700/ICG-EG4 (Figure 3B,D). This would be because the sensitivity of LIGHTVISION is lower than that of the Pearl Imager. On the contrary, these device

properties allowed LIGHTVISION to achieve lower background noise signals and higher TBRs compared to the Pearl Imager (Figure 3E).

From the viewpoint of conjugate chemistry, the chemical characteristics of APC largely depend on the chemical properties of fluorescence dyes.[27] Conjugation of highly charged, large hydrophobic dyes increases liver uptake of APCs, leading to low tumor accumulation that surely compromises therapeutic effects.[28] In contrast, conjugation of hydrophilic and zwitterionic dyes did not alter pharmacokinetics of APCs.[29] IR700 dye is relatively large (molecular weight: 1954.22), yet highly hydrophilic and zwitterionic.[17] Therefore, IR800 dye conjugation in addition to three IR700 dye molecules did not affect *in vivo* pharmacokinetics, resulted in yielding similar therapeutic effects as the parental Tra-IR700 PIT (Figure 4D,E).

Synthesis of dual-conjugated antibody is not cumbersome as a technique, and excitation light of LIGHTVISION (780–800 nm) does not excite IR700 dyes. That is, the tumors can be observed carefully without fear of causing cell damage. Therefore, the addition of IR800 to antibody-IR700 conjugates is useful as a diagnostic tool. Only one big drawback of this method is the extra cost of the additional dyes.

This study has several limitations. For this study, we used a single cell line that does not reflect the full repertoire of cells in a tumor microenvironment. Moreover, the morphology and physiology of mice are quite different from humans, and therefore, clinical studies will be needed to confirm the feasibility of this method. Additionally, in this study, we used LIGHTVISION as an imaging modality, but more than 10 other similar devices are commercially available now. These devices have their own excitation light sources (laser, a lightemitting diode (LED), or xenon), collection optics, and area detectors.[29–31] Different device properties cause different sensitivities and background noise. When using other ICG imaging devices, a standardized preclinical assessment would be required. Therefore, although LIGHTVISION worked very effectively, this does not exclude the possibility that other devices might perform equally.

CONCLUSIONS

The additional conjugation of second NIR dyes to trastuzumab-IR700 conjugates was successfully performed without affecting the efficacy of NIR-PIT. LIGHTVISION, a currently available ICG imaging camera, could visualize NIR-PIT target tumors by detecting the emission fluorescence of IR800. This method would be useful for real-time feedback of tumor locations prior to treatment.

Funding

All authors were supported by the Intramural Research Program of the National Institutes of Health, National Cancer Institute, and the Center for Cancer Research (ZIABC011513, Funder Id: http://dx.doi.org/10.13039/100000054). FFI was also supported with a grant from the National Center for Global Health and Medicine Research Institute, Tokyo, Japan.

REFERENCES

(1). Mitsunaga M; Ogawa M; Kosaka N; Rosenblum LT; Choyke PL; Kobayashi H Cancer cell-selective in vivo near infrared photoimmunotherapy targeting specific membrane molecules. Nat. Med 2011, 17, 1685–1691. [PubMed: 22057348]

(2). Kobayashi H; Choyke PL Near-Infrared Photoimmunotherapy of Cancer. Acc. Chem. Res 2019, 52, 2332–2339. [PubMed: 31335117]

(3). Kobayashi H; Griffiths GL; Choyke PL Near-Infrared Photoimmunotherapy: Photoactivatable Antibody-Drug Conjugates (ADCs). Bioconjugate Chem. 2020, 31, 28–36.

(4). Inagaki FF; Furusawa A; Choyke PL; Kobayashi H Enhanced nanodrug delivery in tumors after near-infrared photoimmunotherapy. Nanophotonics 2019, 8, 1673–1688.

(5). Lum YL; Luk JM; Staunton DE; Ng DKP; Fong WP Cadherin-17 Targeted Near-Infrared Photoimmunotherapy for Treatment of Gastrointestinal Cancer. Mol. Pharmaceutics 2020, 17, 3941–3951.

(6). Kiss B; van den Berg NS; Ertsey R; McKenna K; Mach KE; Zhang CA; Volkmer JP; Weissman IL; Liao Rosenthal EJLC CD47-Targeted Near-Infrared Photoimmunotherapy for Human Bladder Cancer. Clin. Cancer Res 2019, 25, 3561–3571. [PubMed: 30890547]

(7). Nagaya T; Nakamura Y; Okuyama S; Ogata F; Maruoka Y; Choyke PL; Kobayashi H Near-Infrared Photoimmunotherapy Targeting Prostate Cancer with Prostate-Specific Membrane Antigen (PSMA) Antibody. Mol. Cancer Res 2017, 15, 1153–1162. [PubMed: 28588059]

(8). Nagaya T; Nakamura Y; Sato K; Harada T; Choyke PL; Kobayashi H Near infrared photoimmunotherapy of B-cell lymphoma. Mol. Oncol 2016, 10, 1404–1414. [PubMed: 27511870]

(9). Maawy AA; Hiroshima Y; Zhang Y; Heim R; Makings L; Garcia-Guzman M; Luiken GA; Kobayashi H; Hoffman RM; Bouvet M Near infra-red photoimmunotherapy with anti-CEA-IR700 results in extensive tumor lysis and a significant decrease in tumor burden in orthotopic mouse models of pancreatic cancer. PLoS One 2015, 10, No. e0121989.

(10). Vahrmeijer AL; Hutteman M; van der Vorst JR; van de Velde CJ; Frangioni JV Image-guided cancer surgery using near-infrared fluorescence. Nat. Rev. Clin. Oncol 2013, 10, 507–18. [PubMed: 23881033]

(11). Ishizawa T; Bandai Y; Ijichi M; Kaneko J; Hasegawa K; Kokudo N Fluorescent cholangiography illuminating the biliary tree during laparoscopic cholecystectomy. Br. J. Surg 2010, 97, 1369–77. [PubMed: 20623766]

(12). Ishizawa T; Fukushima N; Shibahara J; Masuda K; Tamura S; Aoki T; Hasegawa K; Beck Y; Fukayama M; Kokudo N Real-time identification of liver cancers by using indocyanine green fluorescent imaging. Cancer 2009, 115, 2491–2504. [PubMed: 19326450]

(13). Kitai T; Inomoto T; Miwa M; Shikayama T Fluorescence navigation with indocyanine green for detecting sentinel lymph nodes in breast cancer. Breast Cancer 2005, 12, 211–215. [PubMed: 16110291]

(14). Fujimura D; Inagaki F; Okada R; Rosenberg A; Furusawa A; Choyke PL; Kobayashi H Conjugation Ratio, Light Dose, and pH Affect the Stability of Panitumumab-IR700 for Near-Infrared Photoimmunotherapy. ACS Med. Chem. Lett 2020, 11, 1598–1604. [PubMed: 32832029]

(15). Schindelin J; Arganda-Carreras I; Frise E; Kaynig V; Longair M; Pietzsch T; Preibisch S; Rueden C; Saalfeld S; Schmid B; Tinevez JY; White DJ; Hartenstein V; Eliceiri K; Tomancak P; Cardona A Fiji: an open-source platform for biological-image analysis. Nat. Methods 2012, 9, 676–682. [PubMed: 22743772]

(16). Nagaya T; Okuyama S; Ogata F; Maruoka Y; Choyke PL; Kobayashi H Near infrared photoimmunotherapy using a fiber optic diffuser for treating peritoneal gastric cancer dissemination. Gastric Cancer 2019, 22, 463–472. [PubMed: 30171392]

(17). Sato K; Ando K; Okuyama S; Moriguchi S; Ogura T; Totoki S; Hanaoka H; Nagaya T; Kokawa R; Takakura H; Nishimura M; Hasegawa Y; Choyke PL; Ogawa M; Kobayashi H Photoinduced Ligand Release from a Silicon Phthalocyanine Dye Conjugated with Monoclonal Antibodies: A

Mechanism of Cancer Cell Cytotoxicity after Near-Infrared Photoimmunotherapy. ACS Cent. Sci 2018, 4, 1559–1569. [PubMed: 30555909]

(18). Ogawa M; Kosaka N; Choyke PL; Kobayashi H In vivo molecular imaging of cancer with a quenching near-infrared fluorescent probe using conjugates of monoclonal antibodies and indocyanine green. Cancer Res. 2009, 69, 1268–1272. [PubMed: 19176373]

(19). Sano K; Nakajima T; Miyazaki K; Ohuchi Y; Ikegami T; Choyke PL; Kobayashi H Short PEG-linkers improve the performance of targeted, activatable monoclonal antibody-indocyanine green optical imaging probes. Bioconjugate Chem. 2013, 24, 811–816.

(20). Cherrick GR; Stein SW; Leevy CM; Davidson CS Indocyanine green: observations on its physical properties, plasma decay, and hepatic extraction. J. Clin. Invest 1960, 39, 592–600. [PubMed: 13809697]

(21). Baumann A; Tuerck D; Prabhu S; Dickmann L; Sims J Pharmacokinetics, metabolism and distribution of PEGs and PEGylated proteins: quo vadis? Drug Discovery Today 2014, 19, 1623–1631. [PubMed: 24929223]

(22). Bhattacharyya S; Patel N; Wei L; Riffle LA; Kalen JD; Hill GC; Jacobs PM; Zinn KR; Rosenthal E Synthesis and biological evaluation of panitumumab-IRDye800 conjugate as a fluorescence imaging probe for EGFR-expressing cancers. Medchemcomm 2014, 5, 1337–1346. [PubMed: 25431648]

(23). Rosenthal EL; Warram JM; de Boer E; Chung TK; Korb ML; Brandwein-Gensler M; Strong TV; Schmalbach CE; Morlandt AB; Agarwal G; Hartman YE; Carroll WR; Richman JS; Clemons LK; Nabell LM; Zinn KR Safety and Tumor Specificity of Cetuximab-IRDye800 for Surgical Navigation in Head and Neck Cancer. Clin. Cancer Res 2015, 21, 3658–3666. [PubMed: 25904751]

(24). Rosenthal EL; Moore LS; Tipirneni K; de Boer E; Stevens TM; Hartman YE; Carroll WR; Zinn KR; Warram JM Sensitivity and Specificity of Cetuximab-IRDye800CW to Identify Regional Metastatic Disease in Head and Neck Cancer. Clin. Cancer Res 2017, 23, 4744–4752. [PubMed: 28446503]

(25). Lamberts LE; Koch M; de Jong JS; Adams ALL; Glatz J; Kranendonk MEG; Terwisscha van Scheltinga AGT; Jansen L; de Vries J; Lub-de Hooge MN; Schröder CP; Jorritsma-Smit A; Linssen MD; de Boer E; van der Vegt B; Nagengast WB; Elias SG; Oliveira S; Witkamp AJ; Mali W; Van der Wall E; van Diest PJ; de Vries EGE; Ntziachristos V; van Dam GM Tumor-Specific Uptake of Fluorescent Bevacizumab-IRDye800CW Microdosing in Patients with Primary Breast Cancer: A Phase I Feasibility Study. Clin. Cancer Res 2017, 23, 2730–2741. [PubMed: 28119364]

(26). Miller SE; Tummers WS; Teraphongphom N; van den Berg NS; Hasan A; Ertsey RD; Nagpal S; Recht LD; Plowey ED; Vogel H; Harsh GR; Grant GA; Li GH; Rosenthal EL First-in-human intraoperative near-infrared fluorescence imaging of glioblastoma using cetuximab-IRDye800. J. Neuro-Oncol 2018, 139, 135–143.

(27). Kobayashi H; Choyke PL; Ogawa M Monoclonal antibody-based optical molecular imaging probes; considerations and caveats in chemistry, biology and pharmacology. Curr. Opin. Chem. Biol 2016, 33, 32–8. [PubMed: 27281509]

(28). Sato K; Nagaya T; Nakamura Y; Harada T; Nani RR; Shaum JB; Gorka AP; Kim I; Paik CH; Choyke PL; Schnermann MJ; Kobayashi H Impact of C4′-O-Alkyl Linker on in Vivo Pharmacokinetics of Near-Infrared Cyanine/Monoclonal Antibody Conjugates. Mol. Pharmaceutics 2015, 12, 3303–11.

(29). Sato K; Gorka AP; Nagaya T; Michie M; Nani RR; Nakamura Y; Coble V; Vasalatiy O; Swenson R; Choyke PL; Schnermann MJ; Kobayashi H Role of fluorophore charge on the in vivo optical imaging properties of near-infrared cyanine dye/monoclonal antibody conjugates. Bioconjugate Chem. 2016, 27, 404–13.

(30). Alander JT; Kaartinen I; Laakso A; Pätilä T; Spillmann T; Tuchin VV; Venermo M; Valisuo P A review of indocyanine green fluorescent imaging in surgery. Int. J. Biomed. Imaging 2012, 2012, 1–26.

(31). Zhu B; Sevick-Muraca EM A review of performance of near-infrared fluorescence imaging devices used in clinical studies. Br. J. Radiol 2015, 88, No. 20140547.

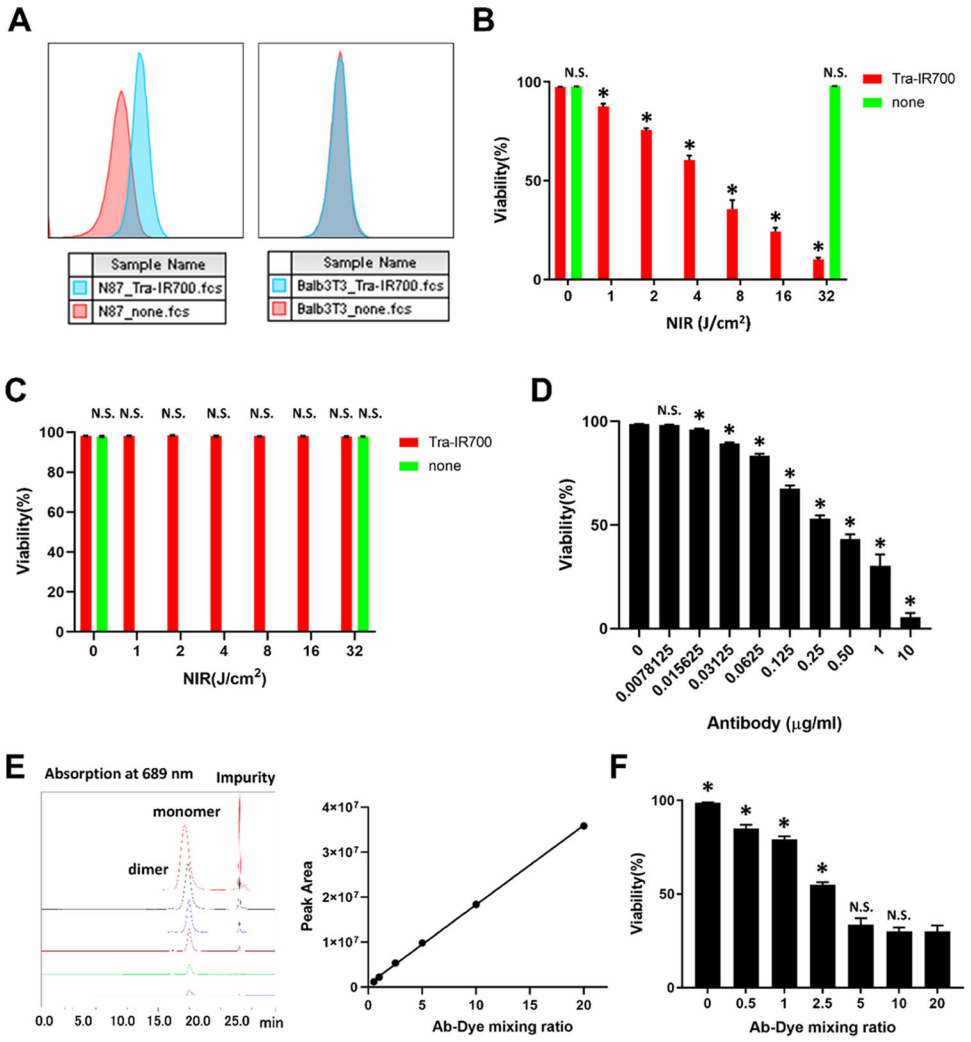

Figure 1.

Factors that determine the therapeutic effect of NIR-PIT: (A) Tra-IR700 binding to N87-GFP/luc cells (left) and Balb/3T3 cells (right). (B) HER2-positive N87-GFP/luc cells were injured by NIR-PIT in a light dose-dependent manner. Cell viability was measured by PI staining. Data are shown as mean ± SEM ($n = 4$, $^*p < 0.05$ *vs* no light exposure group). (C) HER2-negative Balb/3T3 cells were not injured by NIR-PIT. Cell viability was measured by propidium iodide (PI) staining. Data are shown as mean ± SEM ($n = 4$, $^*p < 0.05$ *vs* no light exposure group). (D) APC dose dependence of the therapeutic effect of NIR-PIT *in vitro*. The viability of N87-GFP/luc cells was measured by PI staining. Data are shown as mean ± SEM ($n = 4$, $^*p < 0.05$ *vs* no APC group). (E) SEC analysis of Tra-IR700 at each antibody–dye mixing ratio. Absorption at 689 nm is shown in the left graph. The right graph plots the monomer peak area. (F) Effect of IR700 loading on cell killing. The viability of N87-GFP/luc cells was measured by PI staining. Data are presented as mean ± SEM ($n = 4$, $^*p < 0.05$ *vs* 1:20 mixing ratio group).

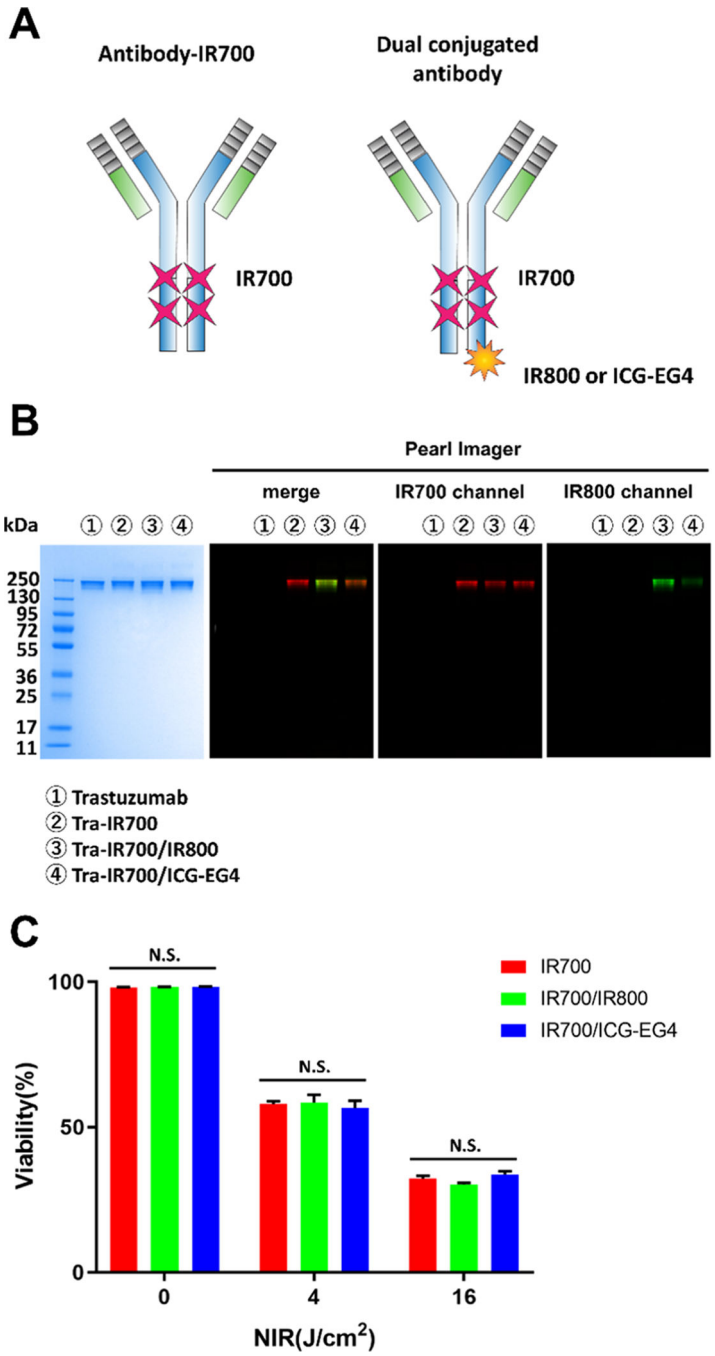

Figure 2.

Characteristics of dual-conjugated antibody: (A) Schema of IR700-conjugated antibody and dual-conjugated antibody. (B) Validation of covalently bound IR700, IR800, and ICG-EG4 to trastuzumab by SDS-PAGE (from left to right: colloidal blue staining, merged fluorescence image, IR700 channel, IR800 channel). (C) Comparison of the *in vitro* therapeutic effect of NIR-PIT. Cell viability was measured by PI staining. In each light exposure dose, there was no significant difference among the Tra-IR700 group, Tra-IR700/IR800 group, and Tra-IR700/ICG-EG4 group. Data are shown as mean ± SEM ($n = 4$).

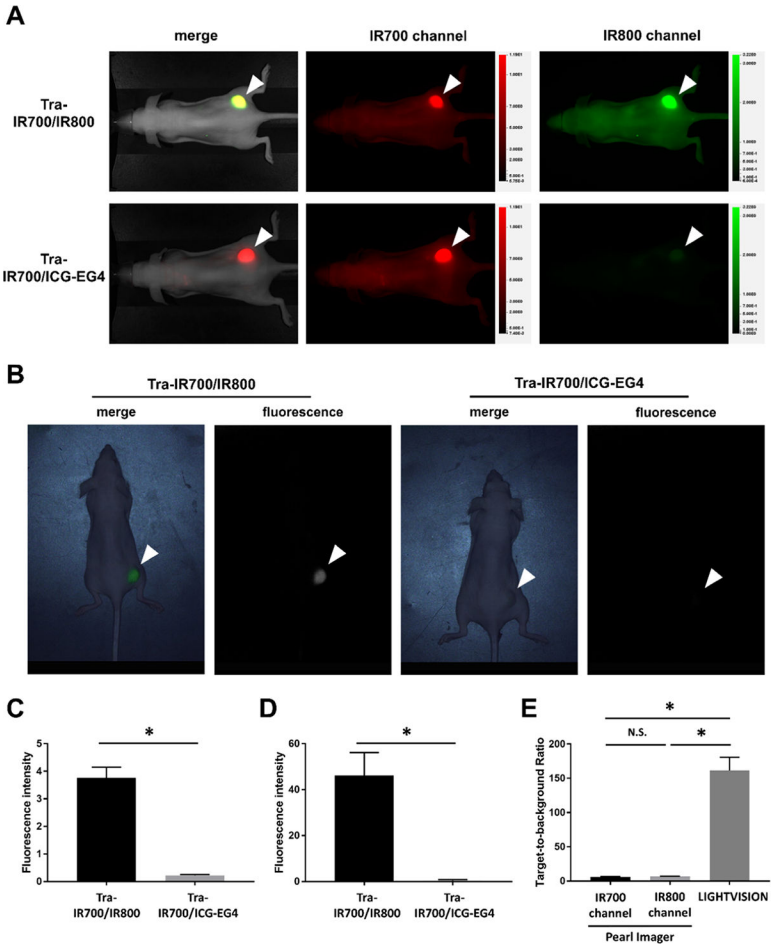

Figure 3.

In vivo imaging of Tra-IR700/IR800 and Tra-IR700/ICG-EG4: (A) Fluorescence images of Tra-IR700/IR800 and Tra-IR700/ICG-EG4 in N87-GFP/luc tumor-bearing mice obtained with the Pearl Imager. A white arrowhead indicates the location of the subcutaneous tumor. (B) Fluorescence images of Tra-IR700/IR800 and Tra-IR700/ICG-EG4 in N87-GFP/luc tumor-bearing mouse obtained by LIGHTVISION. A white arrowhead indicates the location of the subcutaneous tumor. (C) Fluorescence intensity in the tumor region observed with the Pearl Imager. Data are shown as mean ± SEM ($n = 7$, $^*p < 0.05$). (D) Fluorescence intensity in the tumor region observed with LIGHTVISION. Data are shown as mean ± SEM ($n = 7$, $^*p < 0.05$). (E) Target-to-background ratio of N87-GFP/luc tumor in each imaging device. Data are shown as mean ± SEM ($n = 7$, $^*p < 0.05$).

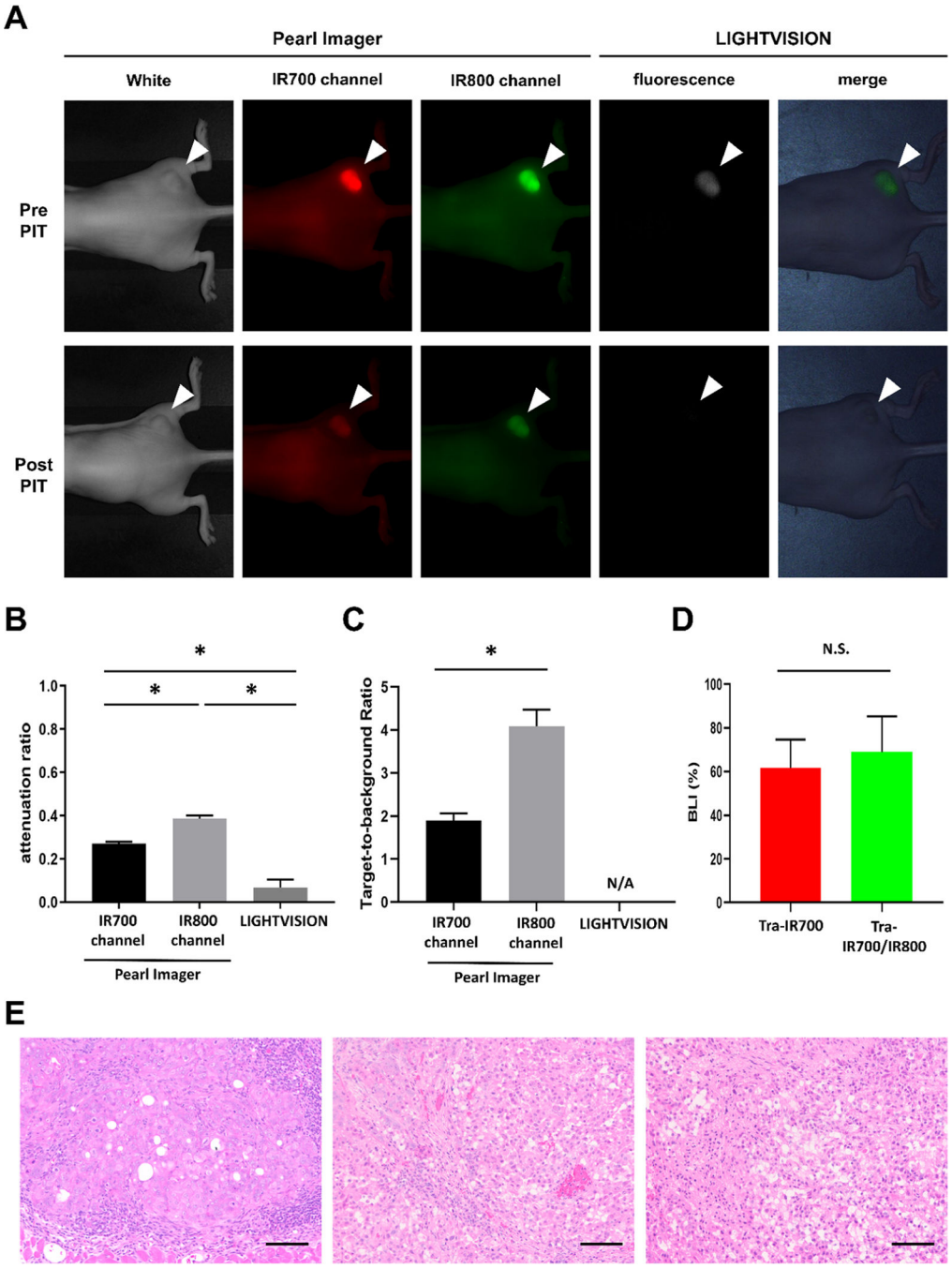

Figure 4.

Changes in fluorescence intensity and early therapeutic effects after NIR-PIT: (A) Fluorescence images of Tra-IR700/IR800 in N87-GFP/luc tumor-bearing mice obtained with the Pearl Imager and LIGHTVISION before and after NIR-PIT. A white arrowhead indicates the location of the subcutaneous tumor. (B) Attenuation ratio of IR700 fluorescence and IR800 fluorescence. Data are shown as mean ± SEM ($n = 7$, $^*p < 0.05$). (C) Target-to-background ratio of N87-GFP/luc tumor in each imaging device after NIR-PIT. Data are shown as mean ± SEM ($n = 7$, $^*p < 0.05$). N/A: not applicable. (D) Attenuation of

bioluminescence in N87-GFP/luc tumor after NIR-PIT. Data are shown as mean ± SEM (n = 10). N/S: not significant. (E) H&E staining of resected tumors (scale bar = 100 μm). Left: no treatment tumor; middle: Tra-IR700 PIT tumor; and right: Tra-IR700/IR800 PIT tumor.

Table 1.

Imaging Modalities[a]

imaging modality	description	clinical use	designed to image	excitation wavelength (nm)	collection wavelength (nm)
LIGHTVISION	in vivo fluorescence imaging system for small animals	no; restricted to research purpose	IRDye700 IRDye800	685 785	720 820
LIGHTVISION	near-infrared fluorescence imaging system, which can be used during surgery	yes; PMDA-approved (available in Japan)	Indocyanine green	780–800	800–850

[a]PMDA, Pharmaceuticals and Medical Devices Agency.